

X-621-74-343

PREPRINT

NASA TM X-70821

IN SITU MEASUREMENTS OF PLASMA DRIFT VELOCITY AND ENHANCED NO^+ IN THE AURORAL ELECTROJET BY THE BENNETT SPECTROMETER ON AE-C

(NASA-TM-X-70821) IN SITU MEASUREMENTS OF
PLASMA DRIFT VELOCITY AND ENHANCED NO^+ IN
THE AURORAL ELECTROJECT BY THE BENNETT
SPECTROMETER ON AE-C (NASA) 15 p HC \$3.25

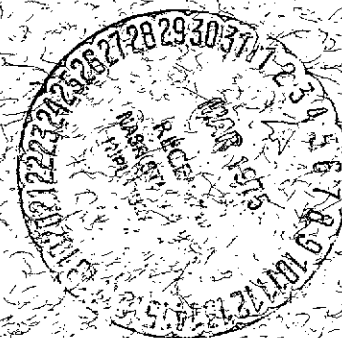
N75-17868

Unclas

CSCL C4A G3/46 10784

HENRY C. BRINTON

NOVEMBER 1974



— GODDARD SPACE FLIGHT CENTER —
GREENBELT, MARYLAND

X-621-74-343

IN SITU MEASUREMENTS OF PLASMA DRIFT VELOCITY
AND ENHANCED NO^+ IN THE AURORAL
ELECTROJET BY THE BENNETT SPECTROMETER ON AE-C

Henry C. Brinton

November 1974

Submitted to Geophysical Research Letters January, 1975

GODDARD SPACE FLIGHT CENTER
Greenbelt, Maryland

IN SITU MEASUREMENTS OF PLASMA DRIFT VELOCITY
AND ENHANCED NO^+ IN THE AURORAL
ELECTROJET BY THE BENNETT SPECTROMETER ON AE-C

Henry C. Brinton

ABSTRACT

Simultaneous measurements of ion composition and plasma drift velocity by the Bennett mass spectrometer on the Atmosphere Explorer-C satellite reveal a direct correlation between enhancements in NO^+ concentration and ion drift velocity in the southern auroral oval. Low altitude (137 to 250 km) nighttime data obtained on October 22, 1974 reveal a region of westward plasma flow at velocities up to 1.3 km/s between 62° and 68° invariant latitude, with corresponding NO^+ enhancements of up to a factor of 25. A narrow region of reverse flow at ~ 0.9 km/s was also measured. These drift observations are consistent with convective flow patterns derived from electric field measurements, and their correlation with NO^+ appears to support the suggestion that NO^+ enhancements would be expected in regions of drift owing to the dependence on ion energy of the reaction $\text{O}^+ + \text{N}_2 \rightarrow \text{NO}^+ + \text{N}$.

PRECEDING PAGE BLANK NOT FILMED

IN SITU MEASUREMENTS OF PLASMA DRIFT VELOCITY
AND ENHANCED NO^+ IN THE AURORAL
ELECTROJET BY THE BENNETT SPECTROMETER ON AE-C

INTRODUCTION

The Bennett ion mass spectrometer on the Atmosphere Explorer-C satellite [Brinton et al., 1973] measures the concentrations of thermal positive ions in the mass range 1 to 72 amu. An additional capability of the instrument is the direct measurement of plasma drift velocity. This note presents simultaneous ion composition and drift data obtained on a low-altitude pass through the southern auroral oval.

DRIFT VELOCITY DETERMINATION

The technique employed applies to data obtained when the spectrometer is pointed in the direction of spacecraft motion. The component of ion drift velocity parallel to the vehicle velocity is determined by measuring the total energy of ions entering the spectrometer and subtracting the energy due to spacecraft motion and vehicle potential. In principle, the method can be extended to data obtained in the spacecraft-spinning mode, thereby yielding information on the vertical component of ion velocity. The measurement of ion energy is possible because the Bennett spectrometer is a relatively low-energy instrument, consisting of a mass analyzer which imparts approximately 60 eV energy to those ions which are instantaneously "resonant," followed by an energy analyzer which permits

only the resonant ions to reach the collector and be measured. (See Brinton et al. [1973] for a more complete instrument description.) Drift velocities are determined by measuring the "harmonic content" of the ion mass spectrum, from which the effective retarding potential and ion entrance energy are evaluated.

Figure 1 is a photograph of the ion spectrum (8 to 72 amu) measured on October 30, 1974 at 165 km altitude for two values of retarding potential, V_s . At the lower value, 53.1 V, "harmonics" [Johnson, 1960] of the fundamental O_2^+ and NO^+ peaks (designated $O_2^+(H)$ and $NO^+(H)$) appear in the spectrum. The amplitudes of these quasi-resonant peaks are extremely sensitive to changes in effective retarding potential, $V_{s\text{ eff}}$, and thus they constitute a convenient monitor of ion entrance energy. The relationship between $V_{s\text{ eff}}$ and entrance energy for NO^+ measurements is given by

$$V_{s\text{ eff}} = V_s + \phi_{sc} - 0.156 (v_{sc} + v_i)^2 \quad (1)$$

where V_s is the commandable retarding potential (volts), ϕ_{sc} is the spacecraft potential (volts), v_{sc} is the spacecraft velocity (km/s), and v_i is the component of ion drift velocity parallel to v_{sc} (km/s). Figure 2 is a plot of the ratio, R , of NO^+ fundamental peak current to its lower harmonic (~ 22 amu) as a function of $V_{s\text{ eff}}$. The drift velocity is determined by computing the value of R for each 8 to 72 amu sweep from the NO^+ and $NO^+(H)$ currents measured by the instrument's on-board digital spectrum processor. The corresponding $V_{s\text{ eff}}$ is then obtained from the Figure 2 data, and by substituting the known values of V_s , ϕ_{sc} , and v_{sc} in equation 1 the ion drift velocity v_i is determined. (Although

at present we use only the lower NO^+ harmonic, its upper harmonic and the harmonics of O_2^+ and O^+ can be employed to increase the spatial resolution of the drift measurement.)

ERROR ANALYSIS

The technique discussed here for deriving drift velocity assumes that no appreciable change in ambient NO^+ concentration occurs between the time of the measurement of NO^+ and its lower harmonic 0.25 s later. Concentration changes will introduce random "noise" in the magnitude of the drift.

The drift data have been derived assuming a constant value of -0.75 V for the spacecraft potential. This value is based on measurements of ϕ_{sc} over many orbits by the cylindrical electrostatic probe on AE-C [Brace et al., 1973]. Dependence on a knowledge of ϕ_{sc} could be eliminated from the drift determination by applying the technique to two ions of different mass such as NO^+ and O^+ .

An estimate of the error in v_i due to ion temperature (T_i) variations indicates that the error is negligible for the temperatures expected. For $T_i \leq 2500 \text{ K}$, the error in v_i is less than 2%; for $T_i = 4000 \text{ K}$, the v_i error is $\sim 20\%$.

Considering all sources of error, the estimated uncertainty in the absolute value of v_i is $\pm 0.2 \text{ km/s}$, while uncertainty in the relative v_i variations is smaller.

Planned improvements in the analysis technique should reduce these uncertainties significantly.

OBSERVATIONS

Ion composition and drift data obtained with the Bennett spectrometer during a perigee pass at high southern latitudes on October 22, 1974 are presented in Figure 3. The track of the subsatellite point for this pass, which occurred largely in the dusk-to-midnight sector, is shown in Figure 4. The day was one of moderate magnetic disturbance with $k_p \sim 3$.

The top panel of Figure 3 is a plot of measured NO^+ concentration versus universal time, from an altitude of approximately 410 km (inbound) through perigee at 137 km to 298 km (outbound). Although measurements of H^+ , He^+ , N^+ , O^+ , N_2^+ and O_2^+ were also obtained, only NO^+ is displayed because it was the dominant ion at low altitude, and ion drift is derived from the NO^+ observations. On both the inbound and outbound portions of the pass O^+ was the dominant ion above about 220 km, with NO^+ dominant below that altitude. As shown in the figure there are three areas in which the NO^+ concentration was considerably enhanced: two regions at ~ 64700 and 65000 s UT are broad, while the third at ~ 64860 s UT is quite narrow.

The data in Figure 3 were obtained with the spectrometer mode in which the retarding potential is switched on successive sweeps through four values. The center panel shows the variation of the ratio R as measured for two of these values. The general decrease in R for $V_s = 57.0$ V in the broad regions of NO^+ enhancement results from a component of ion drift opposite in direction to the

spacecraft velocity. Conversely, the increase in R for $V_s = 53.1$ V, corresponding to the narrow NO^+ enhancement, results from a drift in the direction of spacecraft motion. A composite plot of plasma drift velocity derived from data obtained at all four V_s levels is presented in the lower panel of Figure 3; positive v_i is opposite to v_{sc} , while negative v_i is in the same direction as v_{sc} .

Since Bennett spectrometer efficiency varies with $V_{s \text{ eff}}$ [Brinton et al., 1973], ion concentrations measured in regions of drift require correction. For the highest velocities measured during this pass, NO^+ concentrations in Figure 3 measured in regions of positive v_i should be reduced about a factor of two, while those in regions of negative v_i should be increased by a factor of two.

DISCUSSION

The observed variations in plasma drift velocity and NO^+ concentration appear to be closely correlated with crossings of the auroral oval. On the descending portion of the orbit as the spacecraft moved in a southeast direction in the dusk sector (see Fig. 4), it passed through a rather broad region of westward plasma drift between 64° and 68° invariant latitude (Λ). At about $69^\circ\Lambda$, the highest latitude reached, a narrow region of eastward drift was encountered. Finally, as the spacecraft moved northward near midnight magnetic local time (MLT), it again traversed a broad region of westward drift between 68° and $62^\circ\Lambda$.

We interpret the detection of two regions of westward drift with velocity components of ~ 0.8 km/s along the spacecraft orbit as observations of the auroral

electrojet. Both the magnitude and direction of the observed drift are consistent with thermal plasma convection patterns derived from electric field measurements made with the Injun-5 [Cauffman and Gurnett, 1971] and OGO-6 [Heppner, 1972] satellites. These investigators have reported typical electric field strengths of 50 mV/m in the auroral oval, which are sufficient to produce plasma convection velocities in excess of 0.75 km/s. They have also described abrupt field reversals at auroral latitudes, with corresponding reversals in convection. We interpret the narrow region of eastward drift observed near $69^\circ \Lambda$ and 22 hr MLT as evidence of such a reversal in electric field and ion drift direction. This feature may, alternatively, be associated with the electric field reversal at the Harang discontinuity [Maynard, 1974].

The highest ion drift velocities detected on this pass were confined to a narrow region at approximately $65^\circ \Lambda$ (see Fig. 3). As the satellite crossed this latitude southbound the measured component of v_i was 1.2 km/s, and northbound 0.95 km/s. The locations of these crossings are shown in Figure 4, with the angle between the direction of satellite motion and the tangent to the $65^\circ \Lambda$ circle indicated. Assuming that the horizontal component of ion drift is parallel to these tangents, its magnitude at both locations (as derived from the component measured along the orbital path) is 1.3 km/s. Whether this narrow band of relatively high-velocity ion flow resulted from conditions unique to this pass, or is characteristic of auroral zone drift structure is speculative and will be the subject of further study involving data from other orbits.

The observed enhancements in NO^+ concentration are accompanied by increases in O_2^+ , the second most prevalent ion below 220 km. As shown in Figure 3, simultaneous measurements of ion composition and drift indicate that these molecular ion enhancements occur in the same regions where significant drift velocities are detected, a relationship with interesting implications for high-latitude ion chemistry. This correlation may largely result from the increase with ion kinetic energy of the reaction $\text{O}^+ + \text{N}_2 \rightarrow \text{NO}^+ + \text{N}$, a process suggested by Banks et al. [1974] and Schunk et al. [1974] as contributing to the importance of NO^+ in the high-latitude F-region. Auroral zone enhancements of N_2 density and vibrational temperature are probably also responsible, in part, for the observed NO^+ increases. The importance, particularly at night, of impact ionization due to precipitating particles adds further complication to the picture. A more complete study of the data presented here, supported by simultaneous results from complementary AE-C instruments, should permit assessment of the relative importance of these factors.

REFERENCES

- Banks, P.M., R. W. Schunk, and W. J. Raitt, NO^+ and O^+ in the high-latitude F-region, Geophys. Res. Letters, 1, 239-242, 1974.
- Brace, L. H., R. F. Theis, and A. Dalgarno, The cylindrical electrostatic probes for Atmosphere Explorer-C, -D, and -E, Radio Science, 8, 341-348, 1973.

- Brinton, H. C., L. R. Scott, M. W. Pharo, III, and J. T. Coulson, The Bennett ion-mass spectrometer on Atmosphere Explorer-C and -E, Radio Science, 8, 323-332, 1973.
- Cauffman, D. P. and D. A. Gurnett, Double-probe measurements of convection electric fields with the Injun-5 satellite, J. Geophys. Res., 76, 6014-6027, 1971.
- Heppner, J. P., Electric field variations during substorms: OGO-6 measurements, Planet. Space Sci., 20, 1475-1498, 1972.
- Johnson, C. Y., Bennett radio frequency spectrometer, in The Encyclopedia of Spectroscopy, edited by G. L. Clark, pp. 587-598, Reinhold, New York, 1960.
- Maynard, N. C., Electric field measurements across the Harang discontinuity, J. Geophys. Res., 79, 4620-4631, 1974.
- Schunk, R. W., W. J. Raitt, and P. M. Banks, Effect of electric fields on the daytime high-latitude E- and F-regions, submitted to J. Geophys. Res., November 1974.

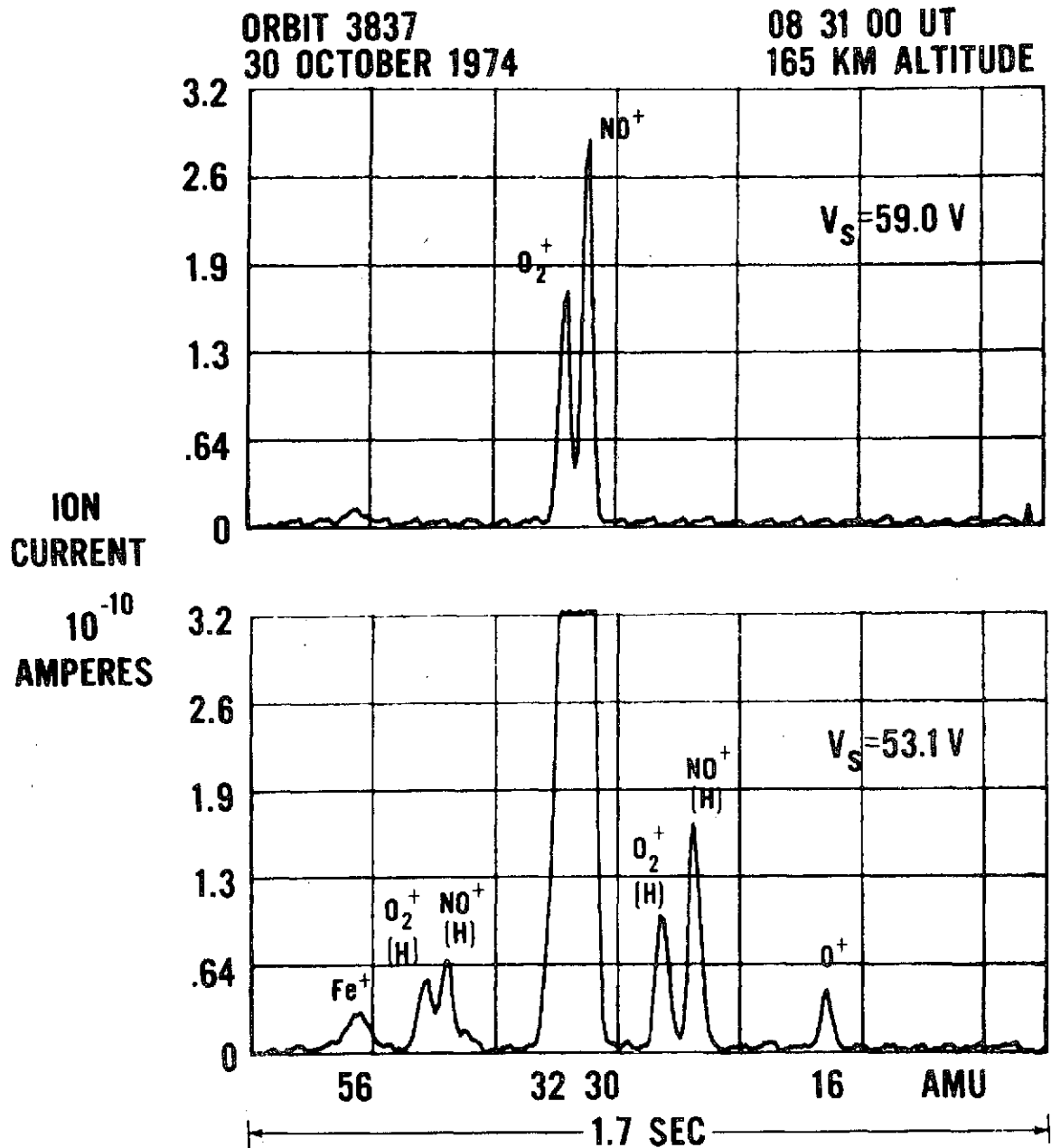


Figure 1. Photograph of the 8 to 72 amu ion spectrum measured by the Bennett spectrometer at 165 km on October 30, 1974. Data obtained at two values of retarding potential, V_s , are shown.

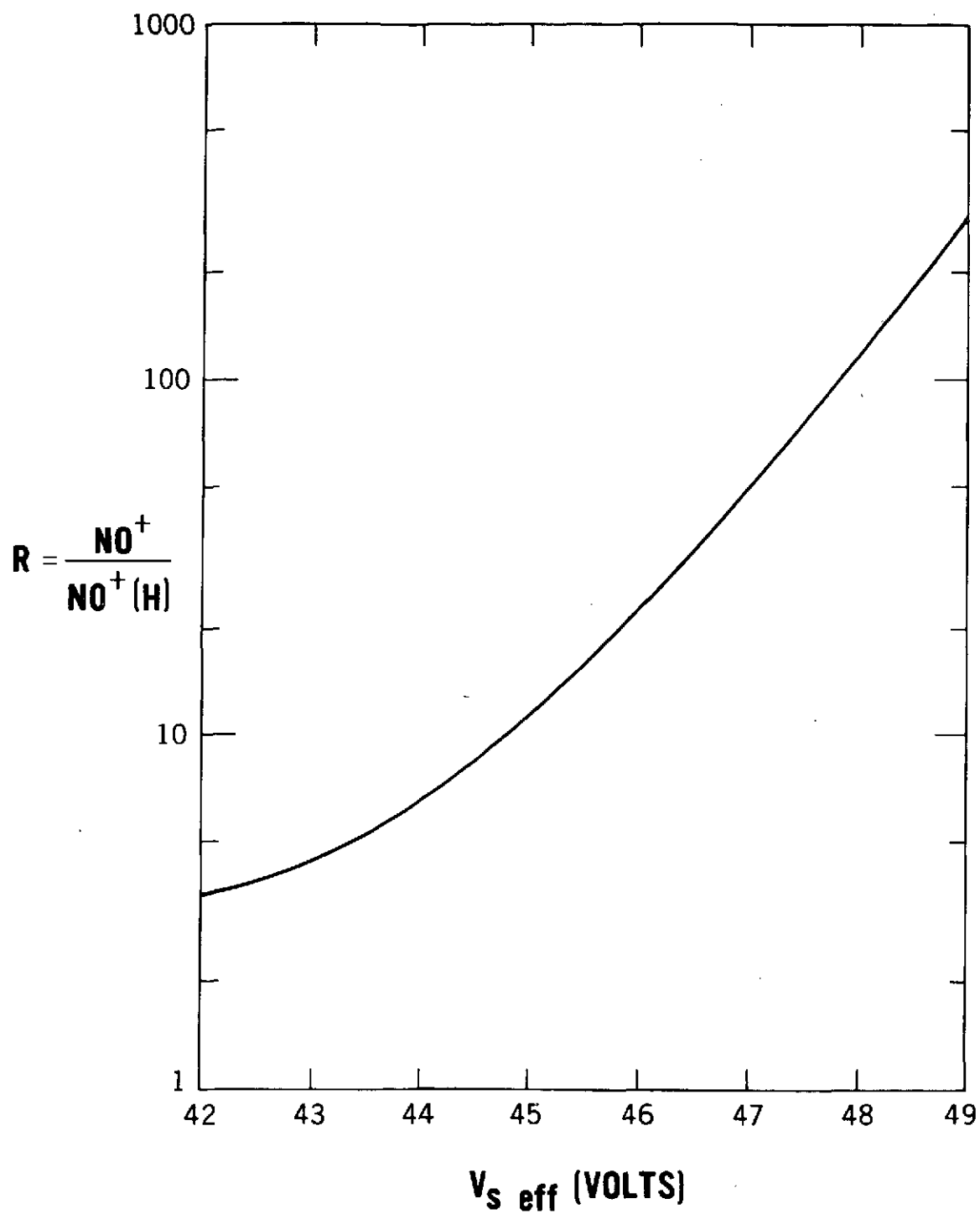


Figure 2. The ratio, R , of NO^+ fundamental and harmonic peak currents as a function of effective retarding potential.

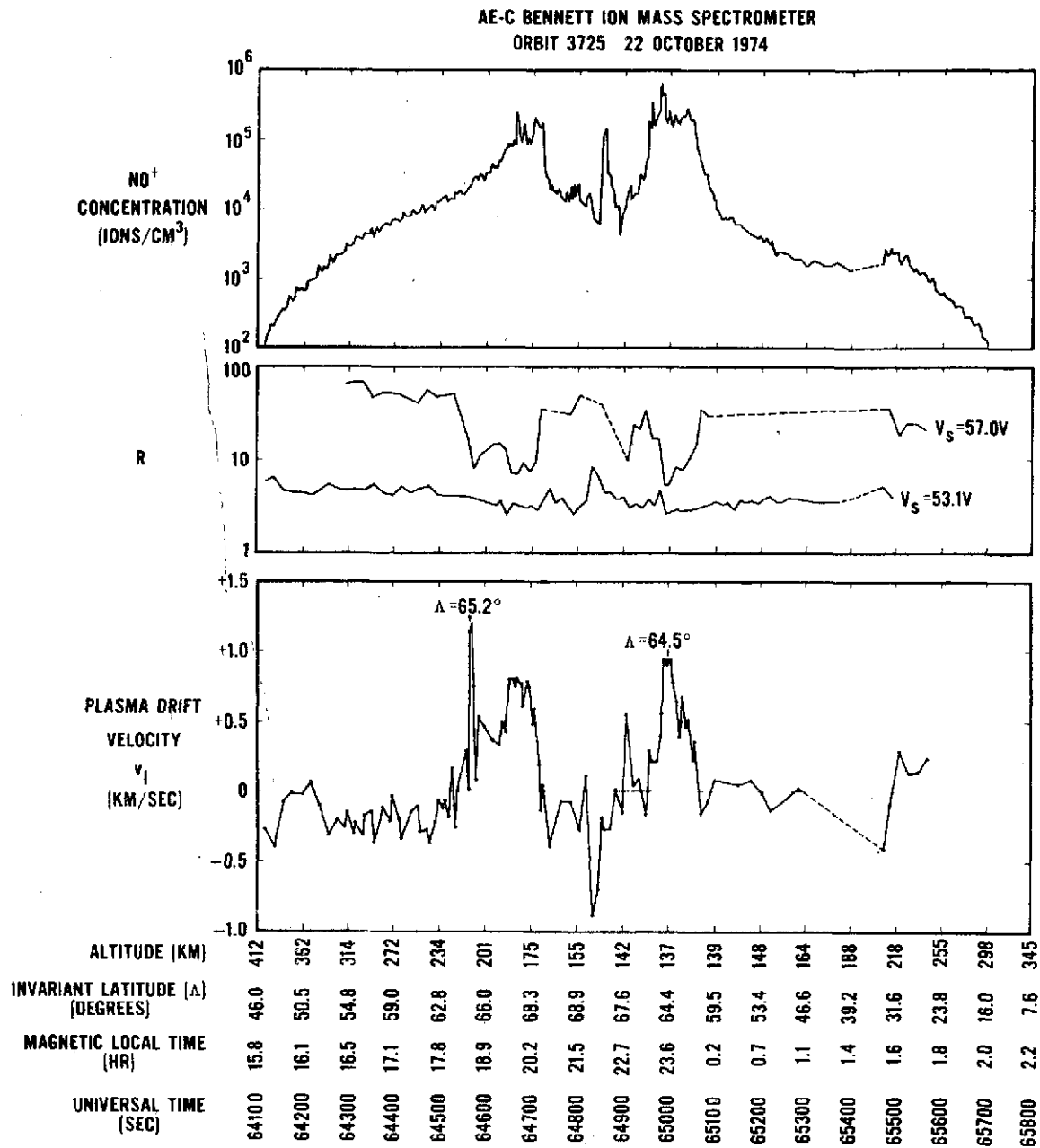


Figure 3. Simultaneous Bennett spectrometer measurements of NO⁺ concentration and plasma drift velocity. The data were obtained during a perigee pass at high southern latitudes on October 22, 1974.

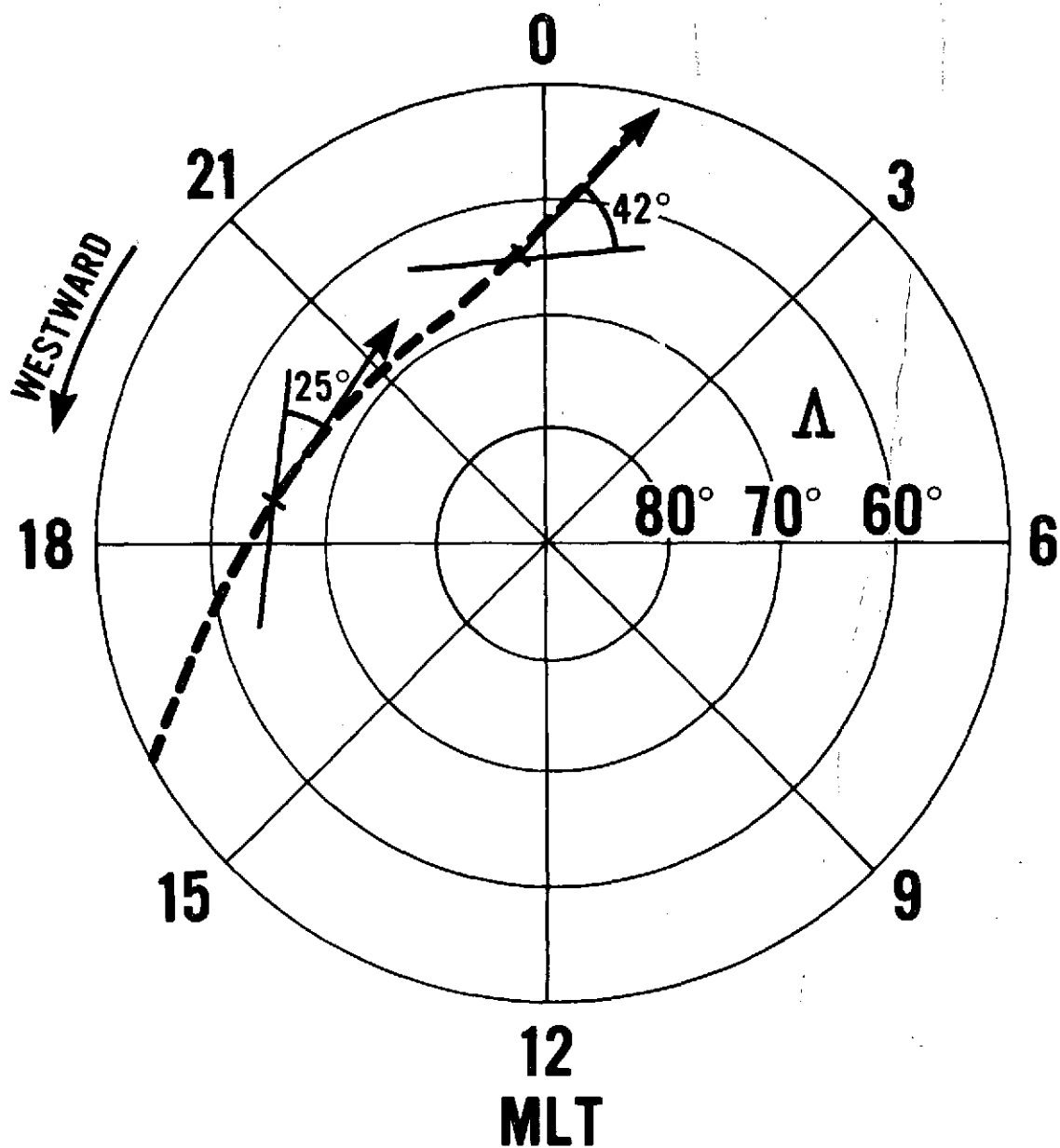


Figure 4. Subsatellite track in magnetic local time and invariant latitude for the orbit on which data in Figure 3 were obtained. Center of figure is the south magnetic pole.